Journal of Theoretical and Applied Mechanics, Sofia, 2013, vol. 43, No. 4, pp. 61–72

THEORETICAL STUDY OF THE EFFECT OF PROBE SHAPE ON ADHESION FORCE BETWEEN PROBE AND SUBSTRATE IN ATOMIC FORCE MICROSCOPE EXPERIMENT*

Li Yang, Junhui Hu, Lingjiang Kong
College of Physics Science and Technology,
Guangxi Normal University, Guilin, 541004, China,
e-mail: guilinderen@126.com

[Received 24 March 2013. Accepted 03 June 2013]

Abstract. The quantitative description of adhesion force dependence on the probe shape is of importance in many scientific and industrial fields. We performed a theoretical study on the influences of the probe shape (the sphere and parabolic probe) on the adhesion force at different humidity in order to elucidate how the adhesion force varied with the probe shape in atomic force microscope manipulation experiment. We found that the combined action of the triple point and the Kelvin radius is the guiding trend of the adhesion force, and these two fundamental parameters are closely related to the probe shape. Meanwhile, the theoretical results demonstrated that the adhesion force are in a good agreement with the experiment data if the van der Waals force is take into account.
Key words: Probe shape, adhesion force, van der Waals force, capillary force, relatively humidity, liquid bridge.

1. Introduction

The atomic force microscope (AFM) has a great impact on various areas, such as nano- metrology [1], materials science [2], surface science and biology [3]. It is a versatile tool for studying nano-materials properties, such as friction and adhesion forces [4]. The quality of image obtained from an AFM is greatly dependent both on the probe shape and physical property, especially the geometry and dimension of the probe end [5]. The chemical

*This work is supported by the National Natural Science Foundation of China under contract Nos 11165004, 81060307, 11164002.
Corresponding author e-mail: guilinderen@126.com

and physical parameters of the probe significantly affect AFM measurements and can reduce resolution [6]. Choosing the correct probe is a crucial part of working on biological samples.

Currently, there are many publications devoted to the probe geometries problem and different models have been established to investigate the adhesion forces between objects with different shapes and a solid plane [7–10]. Most of the previous works focused on the capillary force. Tabrizi et al. [7] numerically calculated the capillary force for a sphere, a cone and a flat cylinder in contact with a planar surface. Their model and experiments showed that the changes of the tip geometry on the sub-10-nm length scale can completely change adhesion force versus humidity curves. Chen et al. [8] studied the influence of the indenter shapes (conical, spherical and truncated conical with a spherical end) on the magnitude of the capillary force in micro-electro-mechanical systems (MEMS). Different dependences of the capillary force on the indenter shapes and the geometric parameters are observed. Butt et al. [9] calculated the capillary forces with three different probe shapes, sphere, cone and cylinder in perfectly wetted surfaces. The results they obtained show that the capillary force and the liquid bridge rupture distance can change fundamentally with different probe shape.

It has already been known that the adhesion force (including van der Waals force, capillary force and electrostatic force) [11] have significantly changes with the different probe shape in AFM experiment, but the details of how the tip shape influences the adhesion force have not been understood clearly. Therefore, a perspective for exhaustive analysis of key parameters is necessary.

In the present paper, the adhesion forces for the sphere probe and the parabolic parabola probe on a substrate in atomic force microscope experiment are theoretically evaluated. The contributions both from the capillary force and the van der Waals force to an adhesion force have been analysed in detail. We found that the triple point and the Kelvin radius that is determined by the probe profile are the key parameters that play a decisive role in adhesion force.

2. Theory

In atomic force microscope (AFM) micro-handling manipulation, the adhesion force results from condensation of water that forms a liquid bridge between the probe and the substrate when the AFM is operated in air [12]. Figure 1 is the schematic diagram of a liquid bridge. R is probe radius, and θ_p and θ_s are the contact angles of the liquid with the probe tip and the substrate, respectively. β is the half-filling angle, x_p is the coordinates of the solid-liquid-vapour contact lines (triple point) with the probe, and D is the probe-substrate

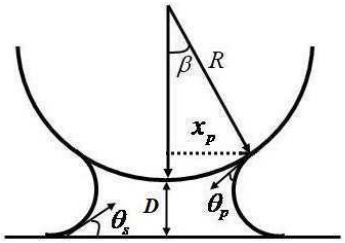

Fig. 1. Liquid bridge between the AFM probe and the substrate

distance. The capillary forces had been calculated numerically with toroidal approximation [13]:

$$F_{cap} = 2\pi\gamma x_p \sin(\beta + \theta_p) + \pi x_p^2 \Delta p. \tag{1}$$

The first term corresponds to the surface tension force and the second denotes the capillary (Laplace) pressure force. Here, γ is the surface tension coefficient. Under thermodynamic equilibrium, the relationship between the relative humidity (RH), the pressure difference Δp across the vapour-liquid interface is related to the mean curvature of the liquid bridge (the Kelvin radius r_k by the Laplace-Young and Kelvin equation [14]:

$$\Delta p = \frac{\gamma}{r_k}. \tag{2}$$

$$r_k = \left(\frac{1}{r_1} + \frac{1}{r_2}\right)^{-1} = \frac{\gamma V_0}{K_B T \ln(RH)}. \tag{3}$$

Here, K_B is the Boltzmann constant, V_0 is the molar volume of liquid, and T is the temperature. The curvature of the liquid bridge is characterized by two radii, which are the azimuthal radius (r_1), and the meridional radius (r_2).

In nanoscale, the van der Waals forces become important at the distances below 10–15 nm and may start to dominate the interactions at these distances, which have been observed at large separations. The van der Waals force F_{vdw} in single medium is given by [15–17]:

$$F_{vdw} = -\frac{H}{6}\left[\frac{R-D}{D^2} + \frac{3R+D}{(D+2R)^2}\right], \tag{4}$$

where R is probe radius and H is the Hamaker constant. To avoid damaging the surface, the separation D for most solid contacts must be kept at least

several tens of angstroms. When there is a liquid bridge appearing in the gap, the van der Waals force between the general probe and the substrate is given by [18]:

$$F_{vdw} = F_{vdw}^{water}\left\{1 - \frac{1}{[1+\frac{y(x)}{D}]^2}\right\} + F_{vdw}^{air}\left\{\frac{1}{[1+\frac{y(x)}{D}]^2}\right\}, \tag{5}$$

where F_{vdw}^{water} and F_{vdw}^{air} are the van der Waals forces with water and air as medium, respectively. They can be calculated by Eq. (4) with different H, R and D. And the r_k, D and β are related by:

$$r_k = \frac{x_p - r_2[1-\cos(\beta+\theta_p)]}{\frac{x_p}{r_2} - 2 + \sin(\beta+\theta_p)}, \tag{6}$$

$$r_{ps} = \frac{D + y(x)}{\cos(\beta+\theta_p) + \cos\theta_s}. \tag{7}$$

For sphere probe, the y(x) and the β are given by:

$$y(x) = \sqrt{R^2 - x^2}, \quad \beta = \arcsin\frac{x}{R}. \tag{8}$$

For parabolic probe, we adopt power function relation:

$$y(x) = kx^n, \quad \beta = \operatorname{arctg}[y'(x)]. \tag{9}$$

The proportional constant k is decided by the shape of the probe tip of the SEM micrograph, the exponent n ($1 \le n \le 4$) is determined by the probe tip apex, and θ is the slope of the probe profile.

The adhesion force is the sum of capillary force and van der Waals force [19]. However, in most previous works [20, 21], the van der Waals force is usually approximated or omitted in the calculation. In our calculation, the analytical expression of the rk and β are derived according to the probe shape, and the van der Waals force is analytically calculated by using Eqs. (4)–(9). Then the adhesion force is precisely calculated by summing the capillary force and the van der Waals force.

3. Results and discussion

The theoretical estimation of the adhesion force is the sum of the capillary force and the van der Waals force, the former is calculated by Eqs. (1)–(3)

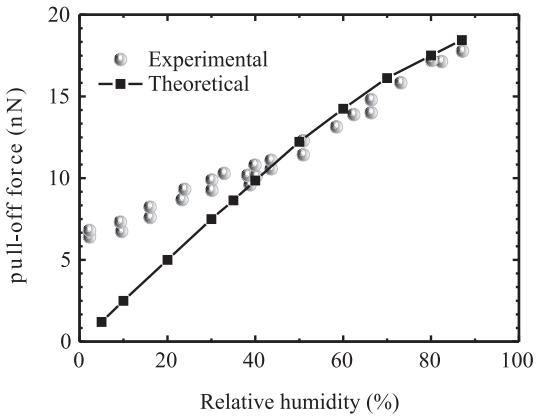

Fig. 2. The experimental data [22] and the theoretical pull-off force for spherical SiO_2 particle on TiO_2 surface versus the RH. ($R = 40$ nm, $\theta_p = 0°$, $\theta_s = 70°$, $D = 0.40$ nm)

while the latter is calculated using Eqs. (4)–(9). In order to illustrate the necessity of the van der Waals force, we performed a comparison between the evaluation and the experimental data for the spherical SiO_2 particle on TiO_2 surface, in which the adhesion force are calculated with and without the van der Waals force, respectively. The experimental process and the experimental results have been described in details in literature [22]. Without considering the van der Waals force, the theoretical capillary force as a function of the RH is calculated by Eqs. (1)–(3) using the parameters from the Ref. 22. The result is plotted in Fig. 2. It can be seen that the capillary force is in a fairly good agreement with the experimental data at $RH \geq 40\%$, but deteriorates when $RH < 40\%$. The large discrepancy between the theoretical results and the experiment data may be attributed to the fact that the adhesion force is dominated by the van der Waals force at a relatively low humidity.

When the van der Waals force is included in the theoretical estimation of the adhesion force, the comparison of the theoretical results with the experiment data is shown in Fig. 3. It is indicated, that the adhesion force between the probe and the substrate increases with the increasing of the RH. In general, the simulation considering the van der Waals force provides a better description for the experimental data than that of considering the capillary force only. Although the van der Waals force is less dominant in the adhesion force, which is about several nano-Newton to tens of nano-Newton, it is should be take into consideration. Therefore, the van der Waals force is contained in our following

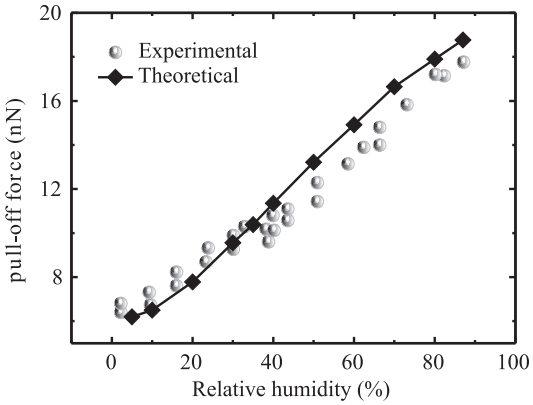

Fig. 3. Adhesion force for SiO_2 particle on TiO_2 surface as a function of RH. $R = 40$ nm, $\theta_p = 0°$, $\theta_s = 70°$, $D = 0.40$ nm [22]. $H = 9.46 \times 10^{-20}$ J in air and $H = 0.69 \times 10^{-20}$ J in water [18]

theoretical estimations.

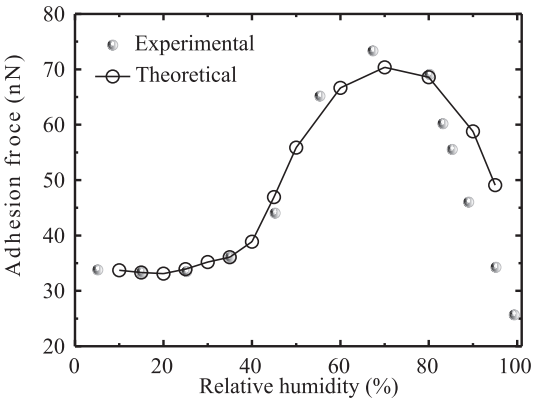

Fig. 4. The adhesion force between the Si_3N_4 probe and SiO_2 surface as a function of RH. $R = 100$ nm, $\theta_p = 60°$, $\theta_s = 0°$, $D = 0.8$ nm [18]

To understand clearly the influence of the tip shape on the adhesion force, we investigate the adhesion force for the sphere probe and the parabola probe on a substrate in the AFM experiment. The comparison between the experimental data and the theoretical estimations results of the adhesion force for parabolic probe as a function of RH are shown in Fig. 4. The adhesion force between the Si_3N_4 probe and SiO_2 surface is calculated to explain the

dependence of adhesion force on the parabolic probe ($k = 1.5 \times 10^{-4}$ nm^{-2}, $n = 3$), which is the optimum function form of probe shape for this experiment defined after many evaluations. In general AFM experiment, the generic sketch of the functional relationship between the pull-off force and the relative humidity (RH) is inverted U-shaped [18, 23]. The force increases steadily at low humidity, rises to a peak at intermediate humidity and falls in high humidity. The results predicted in our model show that the adhesion force grows with the increasing of the RH, which is in accordance with the experiment data shown in the Ref. 18. The good results we obtained might be attributed to the inclusion of the Van der Waals force in the low humidity. Some discrepancies appear at high humidity, possibly due to the influence of the surface roughness which could reduce the Van der Waals force [24–26]. Previous researches have shown that the van der Waals force decreases with increasing roughness, and the roughness weakens the magnitude of the adhesion force interaction compared with smooth surface [27, 28]. For large surface roughness, the radius of curvature of asperity summits should also be taken into account for the estimation of the van der Waals force [29].

It can be seen that the adhesion forces of different probe shapes show different trends in Figs 3 and 4. The main acting force that guided the evolution of the adhesion force should be determined and carefully considered.

The spread of the capillary force and van der Waals force with RH are illustrated in Fig. 5. It is shown that the capillary force grows as the increasing of the RH whereas the van der Waals force displayed contrary tendency. The reason is that the formation of the liquid bridge gradually reduced the van

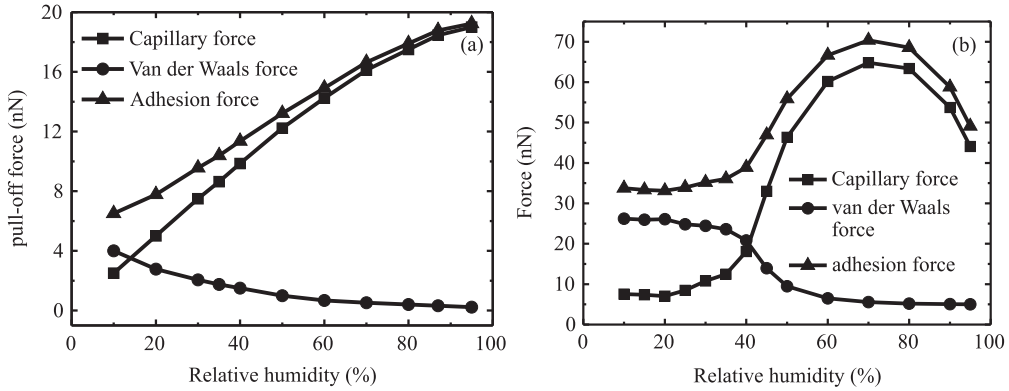

Fig. 5. The adhesion force together with the capillary force and Van der Waals force varying with the RH. (a) The sphere probe. (b) The parabola probe.

der Waals interaction between the particle and the surface [30]. Thus, either of these forces may become dominant dependent on the humidity. At $RH \leq 40\%$, the capillary force and the van der Waals force are in the same order of magnitude. At $RH > 40\%$, the bridge formed the gap fills gradually with water that reduces the van der Waals force from 5.1 nN at a RH of 5% to 0.32 nN at 87% RH. The capillary force interaction is very sensitive to the RH, which is much larger than the van der Waals force under high RH conditions ($RH \geq 40\%$). But the van der Waals force should not be omitted from the force equilibrium if the RH is lower than about 40%. Our results are consistent with the previous experiment measurement [31, 32].

From the previous investigation it can be found that the van der Waals force exhibited nonlinear trends (decreased) with humidity. But it does not play a key role in the adhesion force variation, thus we put the emphasis on the capillary force. According to Eqs. (1)–(3), the numerical magnitude of capillary force is the mutual compensation of these two terms, the capillary (Laplace) pressure force and surface tension force [33]. After numerical, we found that the surface force linearly depended on the humidity, while the capillary pressure force expressed fluctuating characters, which are similar to the adhesion force. The core of the adhesion force is the state parameter which is a relation with the capillary pressure force.

Since the capillary (Laplace) force term predominated in capillary force, whereas the x_p and r_k, are the important factors in the capillary force according to Eq. (2), so two parameters are chosen to be analyzed in detail. The nonlinear variations of x_p (triple point of the liquid bridge) and r_k (Kelvin radius) with

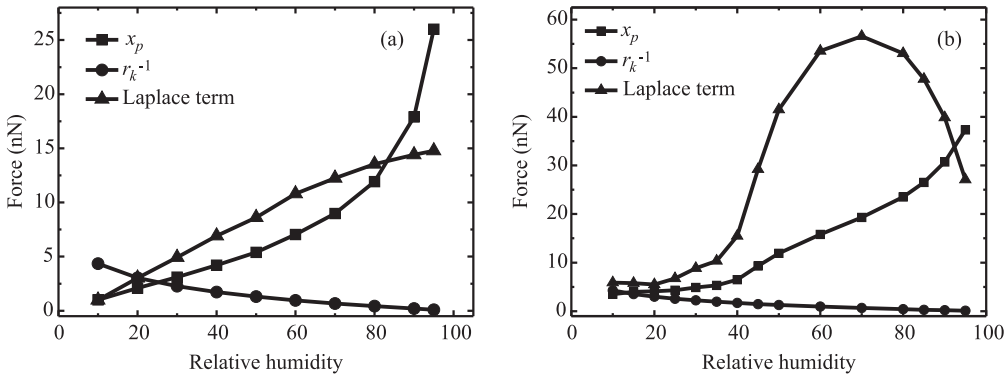

Fig. 6. Effects of x_p and r_k in the capillary pressure force. (a) The sphere probe. (b) The parabola probe

the humidity for two different probe shapes is shown in Fig. 6. It can be seen that x_p increase with the humidity, whereas r_k has an opposite trend. When the positive contribution to the capillary force from increasing x_p is larger than the negative effect from decreasing r_k, the capillary force rises steadily, and vice versa. These two opposite contributions compete to determine whether the trend of capillary force with humidity increment.

At low humidity ($RH < 20\%$), the liquid bridge between the probe and substrate is very small and thin. Thus the value of x_p is less than r_k, the total capillary force trends to decreases.At the intermediate humidity (40% <RH< 70%), the liquid bridge becomes wider and bigger. The increment of x_p is larger than the r_k, so the total capillary force displays dramatic upward. At the high humidity ($RH > 70\%$), the decrement of the r_k surpasses the increment of the x_p, so the total capillary force begin to decrease. On the whole, the capillary force firstly decreased in the low humidity, increased in the intermediate humidity, and finally decreased at high humidity. Since the capillary force is the major determining force, we can see a similar nonmonotonous behaviour for adhesion force in Fig. 5.

With the development of nano-science, materials science and surface science, the various micromanipulation strategies have been proposed, such as electrostatic, vacuum, inertial handling. The use of the adhesion force is considered to be an effective, controllable and secure method in micro-manipulation. It is evident that the pickup manipulation benefits from the increase of adhesion force, and the release manipulation benefits from the decrease of adhesion force. Hence the wider adhesion force range rends to induce better controllability during the AFM manipulation. Comparing to sphere probe, the parabola probe can give a larger interval between the smallest and largest values of adhesion force, which is in a suitable range for practical operation and would be utilized to improve the handling efficiency.

4. Conclusion

In summary, we have theoretically investigated the effect of probe shape on the adhesion force in AFM operation by considering the sphere and parabola probe. In order to clarify the correlation between adhesion force and the probe geometry, the key parameters that influence the adhesion force have been investigated through comparing the theoretical estimations with the experiment data. The numerical simulation shows that the joint action of the triple point and the Kelvin radius are the main factors influencing the adhesion force variation, which are directly related to the probe shape in ambient air.

REFERENCES

[1] Eastman, T., D. M. Zhu. Adhesion Forces Between Surfaces Modified AFM Tips and a Mica Surface. *Langmuir*, **12** (1996), No. 111, 2859–2862.

[2] Thundat, T., X. Y. Zheng, G. Y. Chen, S. L. Sharp, R. J. Warmack, L. J. Schowalter. Characterization of Atomic Force Microscope Tips by Adhesion Force Measurements. *Applied Physics Letters*, **63** (1993), No. 15, 2150–2152.

[3] Binnig, G., C. F. Quate. Atomic Force Microscope. *J. Phys. Rev. Lett.*, **56** (1986), 930–933.

[4] Werf, V. D., K. O. Putman, A. J. Constant, G. De, G. Bart, J. Greve. Adhesion Force Imaging in Air and Liquid by Adhesion Mode Atomic Force Microscopy. *Applied Physics Letters,* **65** (1994), No. 9, 1195–1197.

[5] Thomas, R. C., J. E. Houston, R. M. Crooks, T. S. Kim, T. A. Michalske. Probing Adhesion Forces at the Molecular Scale. *J. Amer. Chem. Soc.*, **117** (1995), No. 13, 3830–3834.

[6] Thundat, T., X. Y. Zheng, G. Y. Chen, R. J. Warmack. Role of Relative Humidity in Atomic Force Microscopy Imaging. *Surface Science Letters*, **294** (1993), 939–943.

[7] Tabrizi, M. F., M. Kappl, H. J. Butt. Influence of Humidity on Adhesion: an Atomic Force Microscope Study. *Journal of Adhesion Science and Technology*, **22** (2008), 181–203.

[8] Chen, S. H., A. K. Soh. The Capillary Force in Micro and Nano Indentation with Different Indenter Shapes. *International Journal of Solids and Structures*, **45** (2008), 3122–3137.

[9] Butt, H. J., M. Kappl. Normal Capillary Forces. *Advances in Colloid and Interface Science*, **146** (2009), 48–60.

[10] Tabrizi, M. F., M. Kappl, Y. Cheng, J. Gutmann, H. J. Butt. On the Adhesion between Fine Particles and Mancontacts: An Atomic Force Microscope Study. *Langmuir*, **22** (2006), 2171–2184.

[11] Quyang, Q., K. Ishida, K. O. Kada. Investigation of Micro Adhesion by Stomic Force Microscopy. *Applied Surface Science*, **169** (2001), 644–648.

[12] Piner, R. D., J. Zhu, F. Xu, S. H. Hong, C. A. Mirkin. "Dip-Pen" Nanolithography. *Science*, **283** (1999), 661–663.

[13] Fisher, R. A. On the Capillary Forces in an Ideal Soil; Correction of Formulae given by W. B. Haines. *Journal of Agricultural Science*, **16** (1926), 492–505.

[14] Yang, L., Y. S. Tu, H. P. Fang. Modelling the Rupture of a Capillary Liquid Bridge between a Sphere and Plane. *Soft Matter*, **6** (2010), 6178–6182.

[15] Vogel, B., H. V. Kanel. AFM Study of Sticking Effects for Microparts Handling. *Wear*, **238** (2000), 20–24.

[16] Dantchev, D., G. Valchev. Surface Integration Approach: A New Technique for Evaluating Geometry Dependent Forces between Objects of Various Geometry and a Plate. *J. Colloid Interface Sci.*, **372** (2012), 148–163.

[17] Valchev, G., D. Dantchev, K. Kostadinov. On the Forces Between Micro and Nano Objects and a Gripper. *International Journal of Intelligent Mechatronics and Robotics (IJIMR)*, **2** (2012), No. 2, 15–33.

[18] Xiao, X., L. Qian. Investigation of Humidity-Dependent Capillary Force. *Langmuir*, **16** (1999), No. 21, 8153–8158.

[19] Lazzer, A. D., M. Dreyer, H. J. Rath. Particle-surface Capillary Forces. *Langmuir*, **15** (1999), 4551–4559.

[20] Jones, R., H. M. Pollock, J. A. S. Cleaver, C. S. Hodges. Adhesion Forces between Glass and Silicon Surfaces in air Studied by AFM: Effects of Relative Humidity, Particle Size, Roughness, and Surface Treatment. *Langmuir*, **18** (2002), No. 21, 8045–8055.

[21] Junno, T., K. Deppert, L. Montelius, L. Samuelson. Controlled Manipulation of Nanoparticles with an Atomic Force Microscope.*J. Appl. Phys. Lett.*,**66** (1995), No. 26, 3627–3629.

[22] Paajanen, M., J. Katainen, O. H. Pakarinen, A. S. Foster. Experiment Humidity Dependency of Small Particle Adhesion on Silica and Titania. *J. Colloid Interface Sci.*, **304** (2006), 518–523.

[23] Arai, F., D. Andou, T. Fukuda. Adhesion Forces Reduction for Micro Manipulation Based on Micro Physics, Proc. IEEE 9$^{\text{th}}$ Annual Int. Workshop on Micro Electro Mechanical Systems, 1996, 354–359.

[24] Li, Q., V. Rudolph, W. Peukert. London-van der Waals Adhesiveness of Rough Particles. *Powder Technology*, **161** (2006), 248–255.

[25] Sedin, D. L., K. L. Rowlen. Adhesion Forces Measured by Atomic Force Microscopy in Humid Air. *Analytical Chemistry*, **72910** (2000), 2183–2189.

[26] Chen, S. C., J. F. Lin. Detailed Modelling of the Adhesion Force between an AFM Tip and a Smooth Flat Surface under Different Humidity Levels. *J. Micromechanics and Microengineering*, **18** (2008), 115006–115013.

[27] Czarnecki, J., T. Dabros. Attenuation of the van der Waals Attraction Energy in the Particle Semi Infinite Medium System Due to the Roughness of the Particle Surface. *J. Colloid Interface Sci.*, **78** (1980), 25–30.

[28] Raymond, R. D., B. Michael, R. W. Lee, C. P. Dennies. Calculation of van der Waals Forces with Diffuse Coatings: Applications to Roughness and Adsorbed Polymers. *J. Adhes. Sci. Technol.*, **80** (2004), No. 5, 365–394.

[29] Rumpf, H. Die Wissenschaft des Agglomerierens. *Chemie Ingenieiur Technik*, **46** (1974), 1–11.

[30] Lennart, B. Hamaker Constants of Inorganic Materials. *J. Adv. Colloid Interface.*, **18** (1997), 125–169.

[31] Jang, J., M. A. Ratner, G. C. Schatz. Atomic-scale Roughness Effect on Capillary Force in Atomic Force Microscopy. *Journal of Physics Chemstry B.*, **110** (2006), 659–662.

[32] Christenson, H. K. Adhesion Between Surfaces in Undersaturated Vapors a Reexamination of the Influence of Meniscus Curvature and Surface Forces. *Journal of Colloid Interface Science*, **121** (1988), No. 1, 170–178.

[33] Aveyard, R., J. H. Clint, J. H. Clint, V. N. Paunov, D. Nees. Capillary Condensation of Vapours between Two Solid Surfaces: Effects of Line Tension and Surface Forces. *Phys. Chem. Chem. Phys.*, **1** (1999), 155–163.